The Statistical Multifragmentation Model with Skyrme effective interactions

B.V. Carlson[1], S.R. Souza[2,3], R. Donangelo[2], W.G. Lynch[4], A.W. Steiner[4], M.B. Tsang[4]

[1]Departamento de Física, Instituto Tecnológico de Aeronáutica - CTA, 12228-900
São José dos Campos, Brazil
[2]Instituto de Física, Universidade Federal do Rio de Janeiro Cidade Universitária,
CP 68528, 21941-972, Rio de Janeiro, Brazil
[3]Instituto de Física, Universidade Federal do Rio Grande do Sul
Av. Bento Gonçalves 9500, CP 15051, 91501-970, Porto Alegre, Brazil
[4] Joint Institute for Nuclear Astrophysics, National Superconducting Cyclotron Laboratory, and the
Department of Physics and Astronomy, Michigan State University, East Lansing, MI 48824, USA

Abstract

The Statistical Multifragmentation Model is modified to incorporate Helmholtz free energies calculated in the finite temperature Thomas-Fermi approximation using Skyrme effective interactions. In this formulation, the density of the fragments at the freeze-out configuration corresponds to the equilibrium value obtained in the Thomas-Fermi approximation at the given temperature. The behavior of the nuclear caloric curve, at constant volume, is investigated in the micro-canonical ensemble and a plateau is observed for excitation energies between 8 and 10 MeV per nucleon. A small kink in the caloric curve is found at the onset of this gas transition, indicating the existence of negative heat capacity, even in this case in which the system is constrained to a fixed volume, in contrast to former statistical calculations.

1 Introduction

Nuclear collisions, at energies starting at a few tens of MeV per nucleon, provide a means to study hot and compressed nuclear matter [1–8]. The determination of the nuclear caloric curve is of particular interest as it allows one to investigate the existence of a liquid-gas phase transition in nuclear matter. Owing to experimental difficulties, conflicting observations have been made in different experimental analyses [9–22], although there have been attempts to harmonize these results [23].

The properties of a fragmenting system in central collisions have been found to be fairly sensitive to the Equation Of State (EOS) in many theoretical studies using dynamical models [1–5]. However, despite the success of statistical multifragmentation models in describing many features of the process of nuclear disassembly [24–26], there has not been much effort to incorporate information based on the EOS in these models. Yet, they have recently been applied to investigate the isospin dependence of the nuclear energy at densities below the saturation value [27–29], in studies that have suggested an appreciable reduction of the symmetry energy coefficient at low densities. Other statistical calculations [30, 31] indicate that surface corrections to the symmetry energy might also explain this behavior. A statistical treatment that consistently includes density effects thus seems appropriate for these studies.

In this work, we modify the Statistical Multifragmentation Model (SMM) [32–34] by including the effects of finite temperature on fragment volumes and free energies using the Thomas-Fermi approximation [35–38] with Skyrme effective interactions [40]. This version of the model is labeled SMM-TF. The internal Helmholtz free energies of the fragments provided by the mean field approximation are fairly sensitive to the Skyrme force used [39], making it possible to investigate whether such statistical treatments might provide information on the EOS. For consistency with the mean field treatment, the equilibrium density of the fragments at the freeze-out stage is also provided by the Thomas-Fermi calculations. Thus, in contrast with the former SMM calculations [41], the hot fragments are allowed to form

at densities below the saturation value. For a fixed freeze-out volume, this leads to a systematic reduction of the free volume, which directly affects the entropy of the fragmenting system, its kinetic energy, and pressure. As a consequence, other properties, such as the caloric curve and particle multiplicities, are also affected.

2 Theoretical framework

In the SMM [32–34], the source is assumed to be formed at a late stage of a reaction and to consist of Z_0 protons and $A_0 - Z_0$ neutrons with total excitation energy E^*. As the system expands, there is a fast exchange of particles within it until a freeze-out configuration is reached, at which point the composition of a set of fragments is well defined. One then assumes that thermal equilibrium has been reached and calculates the properties of the possible fragmentation modes through the laws of equilibrium statistical mechanics. A possible scenario consists in conjecturing that the breakup takes place at constant pressure. In this case, different statistical calculations predict a plateau in the caloric curve [33, 42–47]. The situation is qualitatively different if one assumes that, for a given source, the freeze-out configuration is reached at a fixed breakup volume V_χ. As studied in many places, a monotonous increase of the temperature with the excitation energy occurs in this case [47–49]. In this work, V_χ is kept fixed for all fragmentation modes, and is given by:

$$V_\chi = (1 + \chi)V_0 \ , \tag{1}$$

where V_0 denotes the volume of the system at normal density and $\chi \geq 0$ is an input parameter.

In the micro-canonical version of SMM, the sampled fragmentation modes [34] are consistent with mass, charge, linear momentum and energy conservation. The SMM is then equivalent to a generalized Fermi breakup model [50, 51] in which internal excitation of the fragments is taken into account. The density of states per unit of energy ω_f can be written as

$$
\begin{aligned}
\omega_f \ = \ & \prod_{l=1}^{k} \frac{1}{N_l!} \prod_{j=1}^{n} \left(\frac{V_f}{(2\pi\hbar)^3} \right)^{n-1} \int \prod_{j=1}^{n} d^3p_j \, \delta \left(\sum_{j=1}^{n} \vec{p_j} \right) \\
& \times \int \prod_{j=1}^{n} \left(\rho_j \left(\varepsilon_j \right) d\varepsilon_j \right) \delta \left(\varepsilon_0 - B_0 - E_{c0} - \sum_{j=1}^{n} \left(\frac{p_j^2}{2m_j} + \varepsilon_j - B_j - E_{cj} \right) \right) .
\end{aligned}
\tag{2}
$$

In the above equation, B_0 is the ground state energy of the source and N_l denotes the multiplicity of each type of fragment. B_j corresponds to the binding energy of fragment j, $\vec{p_j}$ represents its linear momentum, ϵ_j^* its excitation energy and $\rho_j \left(\varepsilon_j \right)$ its density of states. The Coulomb repulsion among the fragments is taken into account by the terms E_{c0} and E_{cj} which, together with the self energy contribution included in B_j, gives the Wigner-Seitz [52] approximation discussed in Ref. [32]. V_f denotes the free volume, *i.e.*, it is the difference between V_χ and the volume occupied by all the fragments at freeze-out. As in Ref. [41], henceforth denoted by ISMM here, the fragment binding energy B_j is either taken from experimental values [53] or it is obtained from an extrapolation, if empirical information is not available.

The freeze-out temperature varies from one fragmentation mode f to the other, since it is determined by the constraint of energy conservation. The average temperature is thus calculated, as any other observable O, through the usual statistical average,

$$\langle O \rangle = \frac{\sum_f O_f \omega_f}{\sum_f \omega_f} = \frac{\sum_f O_f \exp(S_f)}{\sum_f \exp(S_f)} \ , \tag{3}$$

where S_f denotes the entropy associated with the mode f. In the SMM, this is calculated through the standard thermodynamical relation
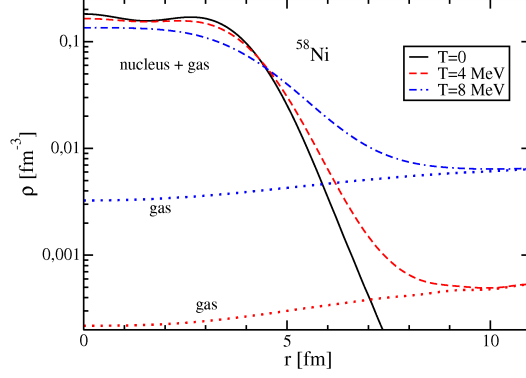
Fig. 1: Nucleus + gas and gas matter distributions of the ^{58}Ni nucleus for three values of the temperature T.

$$S = -\frac{dF}{dT} , \qquad \text{where} \qquad F = E - TS \tag{4}$$

is the Helmholtz free energy. In the following, we write this quantity as

$$F = \sum_{A,Z} N_{A,Z} \left[-B_{A,Z} + f^*_{A,Z}(T) + f^{\text{trans}}_{A,Z}(T) \right] + F_{\text{Coul}} , \tag{5}$$

where the contribution of the internal fragment excitation is related to the density of excited states through

$$f^*_{A,Z}(T) = -T \ln \left[\int_0^\infty d\varepsilon e^{-\varepsilon/T} \rho_{A,Z}(\varepsilon) \right] , \tag{6}$$

and the contribution of the translational motion is given by

$$f^{\text{trans}}_{A,Z} = -T \left[\ln \left(\frac{V_f g_{A,Z} A^{3/2}}{\lambda_T^3} \right) - \frac{\ln(N_{A,Z}!)}{N_{A,Z}} \right] . \tag{7}$$

In the above expression, $\lambda_T = \sqrt{\frac{2\pi\hbar^2}{m_n T}}$, where m_n corresponds to the nucleon mass. A spin multiplicity factor $g_{A,Z}$ is included for light particles but is assumed to be taken into account in $f^*_{A,Z}$ for fragments with $A \geq 5$.

In its original formulation [32], the diluted matter of the SMM is assumed to undergo a prompt breakup in which the fragments collapse to normal nuclear density. The volume they occupy corresponds to V_0, so that the free volume is

$$V_f = \chi V_0 . \tag{8}$$

2.1 The SMM-TF

The Hartree-Fock approximation allows one to calculate the internal free energy and density of a fragment as a function of the temperature. Due to important contributions associated with unbound states at high temperatures, such a treatment is not accurate for $T \gtrsim 4$ MeV, as pointed out by Bonche, Levit, and Vautherin [54]. To extend the calculations to higher temperatures, they observed that there are two solutions of the Hartree-Fock equations for a given chemical potential. One corresponds to a nucleus in equilibrium with its evaporated particles whereas the other is associated with a nucleon gas, as shown in Fig. 1. Thus, in their formalism, the properties of the hot nucleus is obtained by subtracting the
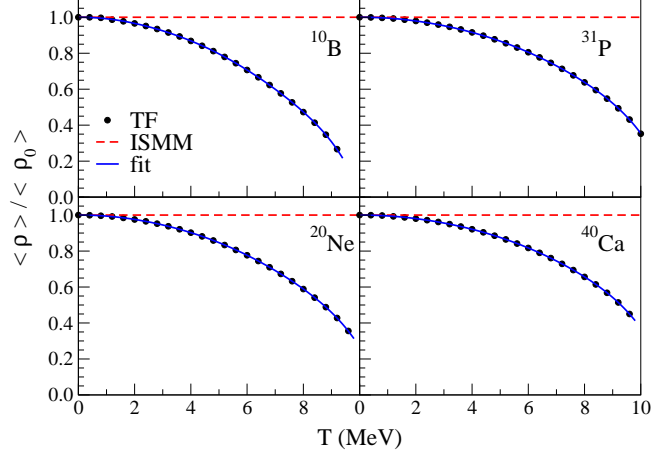
Fig. 2: Ratio between the average equilibrium density of the nucleus at temperature T and the ground state value as a function of the temperature.

thermodynamical potential associated with the nucleon gas from that corresponding to the nucleus in equilibrium with an evaporated gas. Except for the Coulomb energy, there is no interaction between the gas and the nucleus-gas system. This approach was successfully applied by these authors [39, 54] and adapted to the finite temperature Thomas-Fermi approximation by Suraud [38].

The variation of the equilibrium density of a nucleus at temperature T is illustrated in Fig. 2 which shows the ratio between the average density $\langle \rho \rangle$ of several selected light nuclei at temperature T and the corresponding ground state value $\langle \rho_0 \rangle$. We define $\langle \rho \rangle$ as the sharp density which gives the same root mean square radius as the nuclear density obtained in the Thomas-Fermi calculation. One observes that $\langle \rho \rangle$ decreases as one rises the temperature of the nucleus and that it quickly goes to zero as T approaches its limiting temperature, since the nuclear matter tends to move to the external border of the box due to the Coulomb instabilities [38, 39, 54]. In our SMM-TF calculations, we only accept a fragmentation mode if the temperature T is smaller than the limiting temperature of all the fragments of the partition. If this is not the case, the entire partition is discarded and we sample another one.

Thus, the fragment's volume at temperature T is defined as:

$$\frac{V_{A,Z}}{V_{A,Z}^0} = \frac{\langle \rho_0^{A,Z} \rangle}{\langle \rho^{A,Z} \rangle} \, , \tag{9}$$

where $V_{A,Z}^0$ represents the volume of the fragment (A, Z) in the ground state. The free volume V_f then depends on the temperature and is given by

$$V_f (T) = (1 + \chi) V_0 - \sum_{A,Z} V_{A,Z} (T) \, . \tag{10}$$

We also calculate the internal free energies $f_{A,Z}^*$ of the nuclei using the subtracted free energy. The free energies and equilibrium volumes are calculated for the alpha particle and all nuclei with $A \geq 5$.

3 Results and discussion

We apply the SMM-TF model to the breakup of the ^{150}Nd nucleus at a fixed freeze-out density, using $V_\chi / V_0 = 3$. The caloric curve of the system is displayed in Fig. 3. Besides the SMM-TF (circles) and the ISMM (triangles) results, the Thomas-Fermi calculations for the ^{150}Nd nucleus is also shown (dotted line), as well as the Fermi gas (full line) and the Boltzmann (dashed line) expressions. For
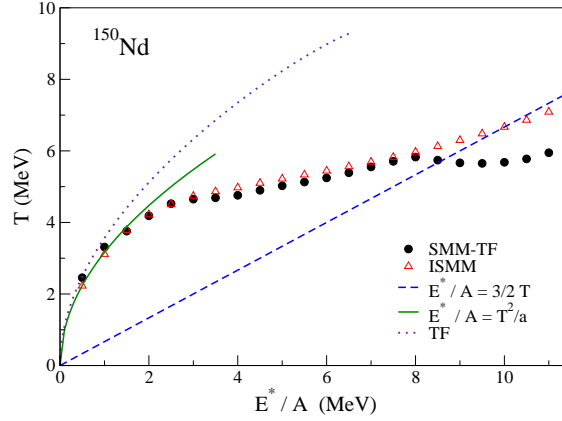
Fig. 3: Caloric curve associated with the breakup of the ^{150}Nd nucleus. For details, see the text.

$E^*/A \lesssim 8.0$ MeV, both SMM calculations agree fairly well for the prediction of the breakup temperatures. However, a kink in the caloric curve is observed at this point, in the case of the SMM-TF, indicating that the heat capacity of the system is negative within a small excitation energy range around this value. Negative heat capacities have been predicted by many calculations and have been strongly debated in the recent literature [33, 42–46, 55–57]. However, this feature is usually observed at the onset of the multifragment emission, *i.e.* at the beginning of the liquid-gas phase transition [33, 45], whereas it appears much later in the present calculation.

In order to understand the qualitative differences between the two SMM approaches, we show, in Fig. 4, the multiplicity of light particles N_{lp} (all particles with $A \leq 4$, except for alpha particles), the alpha particle and the Intermediate Mass Fragment (IMF, $3 \leq Z \leq 15$) multiplicities, as well as the total number of particles N_{total} as a function of the excitation energy. It is important to note that neutrons are included in N_{lp} and N_{total}. One observes a clear disagreement between the two SMM calculations in the prediction of the alpha particles. This is due to the construction of the internal free energies in the ISMM [41], which considers empirical low energy discrete states. Since the first excited state of the alpha particle is around 20 MeV, this strongly increases the free energy at low temperatures, in contrast to the Thomas-Fermi calculation. Except for this difference, the agreement between the model calculations is fairly good, in the case of the other observables, for excitation energies up to $E^*/A \approx 7.5$ MeV. All the multiplicities smoothly increase to approximately this excitation energy. The small discrepancy between N_{total} in the two calculations can be attributed to the differences in the alpha multiplicities. Then, at $E^*/A \approx 7.5$-8.5 MeV, in the SMM-TF calculations, N_α and N_{IMF} reach a maximum and begin to decrease. Another striking feature observed in this picture is the sudden change in the slope of the N_{total} and N_{lp} SMM-TF curves at the same point, not seen in the ISMM results.

Although the Helmholtz free energies of the fragments are somewhat different in both calculations, the differences are not large enough to quantitatively explain this peculiar behavior. The alpha particle is a particular case due to the reasons given above. Thus, this salient feature must be associated with the behavior of the kinetic terms, due to changes in the free volume. The logarithmic volume term in the entropy disfavors partitions with small free volumes. Therefore, the system prefers the emission of very light particles, N_{lp}, (which cannot be excited in our treatment) in order to minimize the reduction of V_f. Nevertheless, this preference is limited by the energy conservation constraint. It is only when the excitation energy becomes sufficiently high that there is enough energy for the system to emit an appreciable number of very light particles. The entropy reaches an approximately constant value in the SMM-TF model for $E^*/A \gtrsim 8.0$ MeV. The large emission of particles which have no internal degrees of freedom prevents the entropy from falling off from this point on, since they do not expand. One should note that the reduction of the complex fragment multiplicities does not mean that the limiting temperature
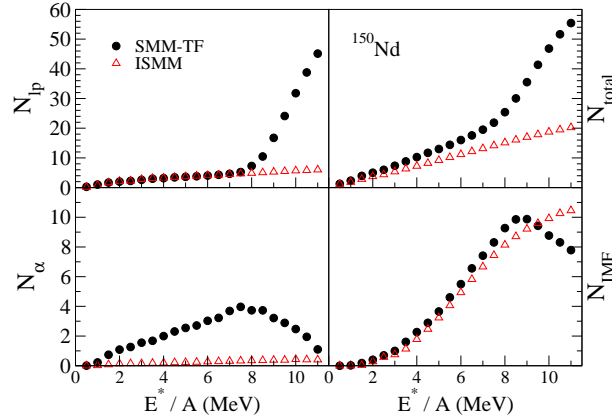
Fig. 4: Average multiplicity of light particles, alpha's, IMF's and total, as a function of the excitation energy.

of the fragments in the different partitions has been reached. In fact, the breakup temperatures obtained in the present calculations are much lower than the limiting temperatures of most nuclei (except for the very asymmetric ones), as may be seen in the examples given in Fig. 2 and in Refs. [38, 39]. This effect on the produced fragments appears at much higher excitation energies. Therefore, the back bending of the caloric curve and the small plateau observed in Fig.3 are strongly governed by the changes in the free volume. Thus, this phase transition at high excitation energy takes place at approximately constant entropy.

Even though the fragments are not directly affected by their limiting temperatures at the excitation energies we consider, the reduction of the entropy associated with the volume affects the fragment species in different ways. Since proton rich nuclei tend to be more unstable, they suffer from the dilatation effects more strongly than the other isotopes. Owing to their larger volumes at a given temperature T, partitions containing proton rich fragments have smaller entropies than the others. Therefore, one expects to observe a reduction in the yields of these fragments. Since the limiting temperatures, as well as the equilibrium density at temperature T, are sensitive to the effective interaction [38, 39], these findings suggest that comparisons with experimental data may provide valuable information on the EOS.

4 Concluding remarks

We have modified the SMM to incorporate the Helmholtz free energies and equilibrium densities of nuclei at finite temperature from the results obtained with the Thomas-Fermi approximation using Skyrme effective interactions. The dilatation of the fragments' volumes has important consequences on the fragmentation modes. For excitation energies larger than approximately 8 MeV per nucleon, it favors a large emission of light particles with no internal degrees of freedom, leading to the onset of a gas transition at excitation energies around this value. The existence of a small kink in the caloric curve, as well as a plateau, for a system at constant volume is qualitatively different from the results obtained in previous SMM calculations where these features were observed only at (or at least at nearly) constant pressure [47].

Since the multiplicities associated with IMF's and light particles are very different in the two statistical treatments for excitation energies larger than 8 MeV per nucleon, we believe that careful comparisons with experimental data may help to establish which treatment is more suited for describing multifragment emission. Furthermore, since the isotopic distribution turns out to be sensitive to the treatment even at lower excitation energies, this suggests that one may learn from the EOS by using different Skyrme effective interactions in the SMM-TF calculations. Particularly, this modified SMM model is appropriate to investigate the density dependence of the symmetry energy discussed recently [27–29].

Acknowledgments

References

[1] P. Danielewicz, R. Lacey, and W. G. Lynch, Science **298**, 1592 (2002).

[2] Bao-An. Li, C. M. Ko, and Z. Ren, Phys. Rev. Lett. **78**, 1644 (1997).

[3] P. Danielewicz, R. A. Lacey, P.-B. Gossiaux, C. Pinkenburg, P. Chung, J. M. Alexander, and R. L. McGrath, Phys. Rev. Lett. **81**, 2438 (1998).

[4] S. R. Souza and C. Ngô, Phys. Rev. C **48**, R2555 (1993).

[5] J. Aichelin, Phys. Rep. **202**, 233 (1991).

[6] V. E. Viola, K. Kwiatkowski, J. B. Natowitz, and S. J. Yennello, Phys. Rev. Lett. **93**, 132701 (2004).

[7] J. P. Bondordf, A. S. Botvina, I. N. Mishustin, and S. R. Souza, Phys. Rev. Lett. **73**, 628 (1994).

[8] W. Bauer, J. P. Bondordf, R. Donangelo, R. Elmér, B. Jakobsson, H. Schulz, F. Schussler, and K. Sneppen, Phys. Rev. C **47**, R1838 (1994).

[9] J. B. Natowitz, R. Wada, K. Hagel, T. Keutgen, M. Murray, A. Makeev, L. Qin, P. Smith, and C. Hamilton, Phys. Rev. C **65**, 034618 (2002).

[10] Y. G. Ma, J. B. Natowitz, R. Wada, K. Hagel, J. Wang, T. Keutgen, Z. Majka, M. Murray, L. Qin, P. Smith, et al., Phys. Rev. C **71**, 054606 (2005).

[11] M. D'Agostino, R. Bougault, F. Gulminelli, M. Bruno, F. Cannata, Ph. Chomaz, F. Gramegna, I. Iori, N. L. Neindre, G. V. Margagliotti, et al., Nucl. Phys. **A699**, 795 (2002).

[12] R. P. Scharenberg, B. K. Srivastava, S. Albergo, F. Bieser, F. P. Brady, Z. Caccia, D. A. Cebra, A. D. Chacon, J. L. Chance, Y. Choi, et al., Phys. Rev. C **64**, 054602 (2001).

[13] X. Campi, H. Krivine, and E. Plagnol, Phys. Lett. **B385**, 1 (1996).

[14] A. Ruangma, R. Laforest, E. Martin, E. Ramakrishnan, D. J. Rowland , M. Veselsky, E. M. Winchester, S. J. Yennello, L. Beaulieu, W.-c. Hsi, et al., Phys. Rev. C **66**, 044603 (2002).

[15] S. Das Gupta, A. Z. Mekjian, and M. B. Tsang, Adv. Nucl. Phys. **26**, 89 (2001).

[16] K. Kwiatkowski, A. S. Botvina, D. S. Bracken, E. Renshaw Foxford, W. A. Friedman, R. G. Korteling, K. B. Morley, E. C. Pollacco, V. E. Viola, and C. Volant, Phys. Lett. **B423**, 21 (1998).

[17] V. Serfling, C. Schwarz, R. Bassini, M. Begemann-Blaich, S. Fritz, S. J. Gaff, C. Groß, G. Immé, I. Iori, U. Kleinevoßet al., Phys. Rev. Lett. **80**, 3928 (1998).

[18] H. F. Xi, G. J. Kunde, O. Bjarki, C. K. Gelbke, R. C. Lemmon, W. G. Lynch, D. Magestro, R. Popescu, R. Shomin, M. B. Tsang, et al., Phys. Rev. C **58**, R2636 (1998).

[19] J. A. Hauger, S. Albergo, F. Bieser, F. P. Brady, Z. Caccia, D. A. Cebra, A. D. Chacon, J. L. Chance, Y. Choi, S. Costa, et al., Phys. Rev. Lett. **77**, 235 (1996).

[20] Y. Ma, A. Siwer, J. Péter, F. Gulminelli, R. Dayras, L. Nalpas, B. Tamain, E. Vient, G. Auger, C. Bacri, et al., Phys. Lett. **B390**, 41 (1997).

[21] L. G. Moretto, R. Ghetti, L. Phair, K. Tso, and G. J. Wozniak, Phys. Rev. Lett. **76**, 2822 (1996).

[22] J. Pochodzalla, T. Möhlenkamp, T. Rubehn, A. Schüttauf, A. Wörner, E. Zude, M. Begemann-Blaich, T. Blaich, H. Emling, A. Ferrero, et al., Phys. Rev. Lett. **75**, 1040 (1995).

[23] J. B. Natowitz, R. Wada, K. Hagel, T. Keutgen, M. Murray, A. Makeev, L. Qin, P. Smith, and C. Hamilton, Phys. Rev. C **65**, 034618 (2002).

[24] J. P. Bondorf, A. S. Botvina, A. S. Iljinov, I. N. Mihustin, and K. Sneppen, Phys. Rep. **257**, 133 (1995).

[25] C. B. Das, S. Das Gupta, W. G. Lynch, A. Z. Mekjian, and M. B. Tsang, Phys. Rep. **406**, 1 (2005).

[26] D. H. E. Gross, Rep. Prog. Phys. **53**, 605 (1990).

[27] A. Le Fèvre, G. Auger, M. L. Begemann-Blaich, N. Bellaize, R. Bittiger, F. Bocage, B. Borderie, R. Bougault, B. Bouriquet, J. L. Charvet, et al., Phys. Rev. Lett. **94**, 162701 (2005).

[28] J. Iglio, D. Shetty, S. J. Yennello, G. A. Souliotis, M. Jandel, A. L. Keksis, S. N. Soisson, B. C. Stein, S. Wuenschel, and A. S. Botvina, Phys. Rev. C **74**, 024605 (2006).

[29] D. V. Shetty, S. J. Yennello, and G. A. Souliotis, Phys. Rev. C **76**, 024606 (2007).

[30] S. R. Souza, M. B. Tsang, R. Donangelo, W. G. Lynch, and A. W. Steiner, Phys. Rev. C **78**, 014605 (2008).

[31] Ad. R. Raduta and F. Gulminelli, Phys. Rev. C **75**, 024605 (2007); **75**, 044605 (2007).

[32] J. P. Bondorf, R. Donangelo, I. N. Mishustin, C. Pethick, H. Schutz, and K. Sneppen, Nucl. Phys. **A443**, 321 (1985).

[33] J. P. Bondorf, R. Donangelo, I. N. Mishustin, and H. Schutz, Nucl. Phys. **A444**, 460 (1985).

[34] K. Sneppen, Nucl. Phys. **A470**, 213 (1987).

[35] M. Brack, C. Guet, and H.-B. Håkansson, Phys. Rep. **123**, 275 (1985).

[36] M. Brack and R. K. Bhaduri, *Semiclassical Physics* (Westview, Boulder, CO, 2003).

[37] E. Suraud and D. Vautherin, Phys. Lett. B **138**, 325 (1984).

[38] E. Suraud, Nucl. Phys. **A462**, 109 (1987).

[39] P. Bonche, S. Levit, and D. Vautherin, Nucl. Phys. **A436**, 265 (1985).

[40] S. R. Souza, B. V. Carlson, R. Donangelo, W. G. Lynch, A. W. Steiner, and M. B. Tsang, Phys. Rev. C **79** (2009) 054602.

[41] W. P. Tan, S. R. Souza, R. J. Charity, R. Donangelo, W. G. Lynch, and M. B. Tsang, Phys. Rev. C **68**, 034609 (2003).

[42] J. B. Elliott and A. S. Hirsch, Phys. Rev. C **61**, 054605 (2000).

[43] P. Chomaz, V. Duflot, and F. Gulminelli, Phys. Rev. Lett. **85**, 3587 (2000).

[44] C. B. Das, S. Das Gupta, and A. Z. Mekjian, Phys. Rev. C **68**, 014607 (2003).

[45] D. Gross, Phys. Rep. **279**, 119 (1997).

[46] S. K. Samaddar, J. N. De, and S. Shlomo, Phys. Rev. C **69**, 064615 (2004).

[47] C. E. Aguiar, R. Donangelo, and S. R. Souza, Phys. Rev. C **73**, 024613 (2006).

[48] S. R. Souza, R. Donangelo, W. G. Lynch, W. P. Tan, and M. B. Tsang, Phys. Rev. C **69**, 031607 (2004).

[49] J. P. Bondorf, A. S. Botvina, and I. N. Mishustin, Phys. Rev. C **58**, R27 (1998).

[50] E. Fermi, Prog. Theor. Phys. **5** (1950) 570.

[51] M. Epherre and E. Gradsztajn, J. de Phys. **28** (1967) 745.

[52] E. Wigner and F. Seitz, Phys. Rev. **46**, 509 (1934).

[53] G. Audi and A. H. Wapstra, Nucl. Phys. **A595**, 409 (1995).

[54] P. Bonche, S. Levit, and D. Vautherin, Nucl. Phys. **A427**, 278,296 (1984).

[55] K. Michaelian and I. Santamaría-Holek, Eur. Phys. Lett. **79**, 43001 (2007); **82**, 43002 (2008); **82**, 43004 (2008).

[56] D. Lynden-Bell and R. Lynden-Bell, Eur. Phys. Lett. **82**, 43001 (2008).

[57] F. Calvo, D. Wales, J. Doye, R. Berry, P. Labastie, and M. Schmidt, Eur. Phys. Lett. **82**, 43003 (2008).